Anomalous expansion and phonon damping due to the Co spin-state transition in $RCoO_3$ (R=La, Pr, Nd, and Eu)

K. Berggold,[1] M. Kriener,[1,2] P. Becker,[3] M. Benomar,[1] M. Reuther,[1] C. Zobel,[1] and T. Lorenz[1,*]
[1]*II. Physikalisches Institut, Universität zu Köln, Zülpicher Strasse 77, 50937 Köln, Germany*
[2]*Department of Physics, Graduate School of Science, Kyoto University, Kyoto 606-8502, Japan*
[3]*Institut für Kristallographie, Universität zu Köln, Zülpicher Strasse 49b, 50674 Köln, Germany*
(Received 25 June 2008; published 3 October 2008)

We present a combined study of the thermal expansion and the thermal conductivity of the perovskite series $RCoO_3$ with R=La, Nd, Pr, and Eu. The well-known spin-state transition in $LaCoO_3$ is strongly affected by the exchange of the R ions due to their different ionic radii, i.e., chemical pressure. This can be monitored in detail by measurements of the thermal expansion, which is a highly sensitive probe for detecting spin-state transitions. The Co ions in the higher spin state act as additional scattering centers for phonons, therefore suppressing the phonon thermal conductivity. Based on the analysis of the interplay between spin-state transition and heat transport, we present a quantitative model of the thermal conductivity for the entire series. In $PrCoO_3$, an additional scattering effect is active at low temperatures. This effect arises from the crystal-field splitting of the $4f$ multiplet, which allows for resonant scattering of phonons between the various $4f$ levels.

DOI: 10.1103/PhysRevB.78.134402 PACS number(s): 65.40.De, 65.40.G−, 72.20.−i

I. INTRODUCTION

Cobalt compounds are of particular interest due to the possibility that Co ions can exhibit different spin states and hence the occurrence of temperature-driven spin-state transitions. The most prominent example is $LaCoO_3$, which has been intensively studied and controversially debated for more than 50 years; see, e.g., Refs. 1–9. The Co^{3+} ions in $LaCoO_3$ feature a $3d^6$ configuration, which in principle can occur in three different spin states: nonmagnetic low-spin (LS) ($t_{2g}^6e_g^0$, S=0), intermediate-spin (IS) ($t_{2g}^5e_g^1$, S=1) or high-spin (HS) states ($t_{2g}^4e_g^2$, S=2). It is generally agreed that the Co^{3+} ions in $LaCoO_3$ realize the LS state at low temperatures. Above approximately 25 K, a higher spin state either IS or HS becomes thermally populated affecting various physical properties, e.g., the magnetic susceptibility χ or the thermal expansion α, which both exhibit pronounced maxima in their temperature dependencies.[10,11] The susceptibility is obviously affected because the excited spin state either IS or HS induces a strong increase in the magnetization above 25 K. The thermal expansion is affected due to the different ionic radii of the smaller LS-Co^{3+} with empty e_g orbitals and the larger IS- or HS-Co^{3+} ions with partially filled e_g orbitals. The spin-state transition can be well described in a LS-IS scenario, i.e., the excited spin state is the IS state with a constant energy gap of Δ_{Co}=185 K (Refs. 10 and 11). However, more recent investigations show that a LS/HS model including spin-orbit coupling is more reasonable.[12–14] A consequence of the latter model is a temperature-dependent energy gap $\Delta_{Co}(T)$, which strongly increases with increasing temperature.[13] Such an increase in Δ_{Co} may arise from a negative cooperative effect between Co ions in the excited spin state.[15]

The spin-state transition in $LaCoO_3$ is strongly affected by both heterovalent and isovalent dopings on the La site. The former possibility causes hole doping and chemical pressure and suppresses the spin-state transition due to the implementation of Co^{4+} ions.[16,17] The latter one, i.e., chemical pressure without changing the Co valence, is usually realized by introducing trivalent rare-earth ions R^{3+}. In $RCoO_3$ the spin-state transition is not suppressed but its onset is shifted to higher temperature. The energy gap between the LS and the excited spin state increases from about Δ_{Co}=185 K for R=La to $\gtrsim$2000 K for R=Eu.[11] Moreover, due to the decreasing ionic radius of the lanthanide series, the structure changes from rhombohedral in $LaCoO_3$ to orthorhombic for R=Pr, Nd, and Eu. Recently, it has been reported that the low-temperature thermal conductivity of $LaCoO_3$ is also very anomalous.[18,19] This behavior has been qualitatively attributed to the onset of the spin-state transition. However, a quantitative analysis of the anomalous thermal conductivity of $LaCoO_3$ has not been presented yet.

The aim of this paper is to develop a consistent picture of the influence of the spin-state transition on the thermal conductivity. Therefore, we measured the thermal conductivity $\kappa(T)$ of the series $RCoO_3$ with R=La, Pr, Nd, and Eu. Moreover, we studied the thermal expansion $\alpha(T)$, which is a very sensitive probe to investigate spin-state transitions and also crystal-field excitations and their coupling to the lattice. In the quantitative analysis of our data, we will consider both models of the spin-state transition, which are favored for $LaCoO_3$ in the literature, i.e., we will consider the LS-IS scenario with a constant Δ_{Co} and the more recently proposed spin-orbit coupled HS (SOcHS) model with a temperature-dependent energy gap $\Delta_{Co}(T)$.

II. EXPERIMENT

All $RCoO_3$ crystals have been grown in a floating-zone image furnace. We examine five different $LaCoO_3$ crystals identical to those used in Ref. 19, where details of the sample preparation and characterization are given. For $EuCoO_3$ this information can be found in Ref. 11. The $NdCoO_3$ and $PrCoO_3$ single crystals have been grown in the same way as those of $LaCoO_3$ and $EuCoO_3$. Characteristic properties of all crystals are listed in Table I. The thermal-conductivity

TABLE I. Characteristic properties of the investigated crystals. Here, T_{on} denotes the onset temperature of the spin-state transition, Δ_{Co} is the energy gap between the LS ground and the excited spin states (either IS or HS), and γ is related to their ionic radii difference (see text). Due to the large T_{on} of $EuCoO_3$, we can only give lower limits for the values of γ and Δ_{Co} as it was also the case in the related analysis of the magnetic susceptibility (Ref. 11). The last three columns give the room-temperature values of the thermopower S_{RT}, which for the $LaCoO_3$ crystals have been taken from Ref. 19 (as discussed there, the different values of S_{RT} arise from weak oxygen off stoichiometries), and the crystal dimensions (sample cross section A and sample length L), which are important for the measurements of κ (the cross section of S5 is an approximate value since it is not of rectangular shape).

Sample	T_{on} (K)	Δ_{Co} (K)	γ (%)	S_{RT} (μV/K)	A (mm^2)	L (mm)
$LaCoO_3$(S1)	25	185	0.7	−700	0.8×1.5	3.7
$LaCoO_3$(S2)				1000	1.1×0.8	2.3
$LaCoO_3$(S3)				−600	1.4×0.8	3.4
$LaCoO_3$(S4)				1000	0.8×1.4	2.6
$LaCoO_3$(S5)				−300	2.3	4.7
$PrCoO_3$	175	1200	2.8	−400	1.0×3.8	2.5
$NdCoO_3$	230	1700	4.8	−400	1.7×2.0	2.8
$EuCoO_3$	400	≳2000	≳10	−500	0.3×0.85	2.0

measurements have been performed by a standard steady-state method using a differential Chromel-Au+0.07% Fe thermocouple.[20] The thermal expansion below ≈200 K was measured using a home-built high-resolution capacitance dilatometer;[21] whereas the high-temperature measurements 135 K≲T≲670 K were performed using a commercial inductive dilatometer (TMA 7, Perkin-Elmer).

III. RESULTS AND DISCUSSION

A. Thermal expansion

In Fig. 1(a) we show the thermal-expansion coefficients $\alpha(T)=1/L(\partial L/\partial T)$ of $RCoO_3$. The low-temperature results of $LaCoO_3$ and $EuCoO_3$ were already discussed in detail in Ref. 10 and 11. The thermal expansion consists of a phononic part and a Schottky contribution caused by the thermal population of the e_g orbitals of the Co^{3+} ions, i.e., $\alpha=\alpha_{ph}+\alpha_{Sch}$. The latter contribution causes the large maximum at 50 K in $LaCoO_3$. To further analyze the data we subtract α_{ph}, which we estimate using a Debye function with the Debye temperature Θ_D=600 K of $LaCoO_3$ (Ref. 22). Here, we used the same Θ_D for the various cobaltates but sample-dependent prefactors determined by scaling the Debye function to the low-temperature data of each compound. As an example, we show α_{ph} for $NdCoO_3$ in Fig. 1(a); α_{ph} of $EuCoO_3$ ($PrCoO_3$; not shown) is slightly larger (smaller). Since a clear separation of α_{ph} and α_{Sch} is not possible for the low-temperature data of $LaCoO_3$, we used α_{ph} of $EuCoO_3$ also for $LaCoO_3$. The resulting α_{Sch} of all crystals are shown in Fig. 1(b). We note that in particular for $PrCoO_3$ and $NdCoO_3$, the spin-state transition is seen much better in the thermal-expansion data than in the magnetic susceptibility. The reason is that α_{Ph} is rather small compared with the total thermal expansion; whereas χ is dominated by the large contribution of the $4f$ moments of the Pr^{3+} and Nd^{3+} ions, respectively, which makes a further analysis rather uncertain. The metal-insulator (MI) transitions occurring above about 500 K, see, e.g., Refs.

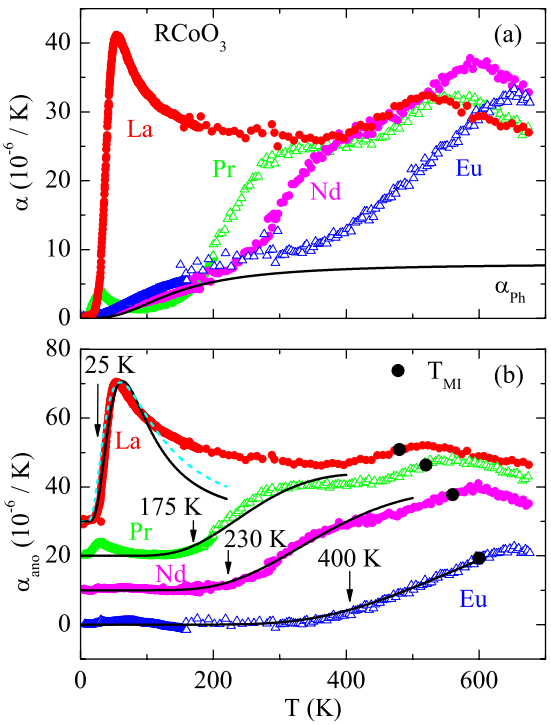

FIG. 1. (Color online) (a) Thermal expansion of $RCoO_3$ with R=La, Pr, Nd, and Eu. The solid line is the estimated phonon contribution of $NdCoO_3$(see text). (b) Anomalous part of the thermal expansion obtained by subtracting the phononic background. For clarity the different data sets are offset by 1×10^{-5}/K with respect to each other. The arrows signal the approximate onset temperature of the spin-state transition, and the solid circles denote the metal-insulator transition temperature estimated from resistivity measurements for each compound. The solid lines are fits of the respective Schottky anomalies [see Eqs. (1) and (2)] assuming a constant energy gap Δ_{Co} between the different spin states of Co^{3+}. The dashed line for $LaCoO_3$ is a similar fit using $\Delta_{Co}(T)$ obtained from the magnetic susceptibility (see text).

11 and 23, also cause anomalies in $\alpha(T)$. The solid circles in Fig. 1(b) signal the transition temperatures T_{MI}, which have been determined from resistivity measurements in our crystals (not shown).

Within the LS/IS scenario with a constant Δ_{Co}, $\alpha_{\mathrm{Sch}}(T)$ is given by

$$\alpha_{\mathrm{Sch}}(T) = \gamma \frac{\Delta_{\mathrm{Co}}}{T^2} \frac{\nu \exp(-\Delta_{\mathrm{Co}}/T)}{[1+\nu \exp(-\Delta_{\mathrm{Co}}/T)]^2}, \quad (1)$$

where $\nu=3$ is the degeneracy of the excited spin state and γ is a measure of the ionic radii difference of the Co^{3+} in the LS and in the excited spin state.[10] Moreover, γ is related to the uniaxial pressure dependence of Δ_{Co} via $\gamma = k_B/V_{\mathrm{fu}}(\partial\Delta_{\mathrm{Co}}/\partial p_\alpha)$, where k_{B} is Boltzmann's constant, $V_{\mathrm{fu}} \simeq 56$ Å^3 is the volume per formula unit, and p_α means uniaxial pressure along the direction of which α is measured.[24,25] To get the hydrostatic pressure dependence one has to use the volume expansion, which in the case of the twinned $R\mathrm{CoO}_3$ single crystals is given by 3α. The corresponding fit of α of LaCoO_3 (already presented in Ref. 10) is shown by the solid line in Fig. 1(b). The fit parameters are $\Delta_{\mathrm{Co}}=185$ K and $\gamma=0.7\%$ giving a hydrostatic pressure dependence $\partial(\ln \Delta_{\mathrm{Co}})/\partial p_{\mathrm{hydr}} \simeq 45\%/\mathrm{GPa}$ in agreement with the increase in Δ_{Co} of 42% obtained from measurements of χ under 1.1 GPa (Ref. 26).

For the SOcHS model one has to consider the temperature dependence of Δ_{Co} (Ref. 13), which can be calculated from the measured $\chi(T)$ (Ref. 11). For LaCoO_3, this yields a linear increase $\Delta_{\mathrm{Co}}^{\mathrm{HS}}(T)=\Delta_{\mathrm{Co}}^0+aT$ with $\Delta_{\mathrm{Co}}^0=135$ K and $a=1.66$ in the temperature range almost up to the MI transition. Using this $\Delta_{\mathrm{Co}}^{\mathrm{HS}}(T)$ in the partition sum, Eq. (1) modifies to

$$\alpha_{\mathrm{Sch}}(T) = \gamma^{\mathrm{HS}} \frac{\Delta_{\mathrm{Co}}^0}{T^2} \frac{\nu \exp[-(\Delta_{\mathrm{Co}}^0 + aT)/T]}{\{1+\nu \exp[-(\Delta_{\mathrm{Co}}^0 + aT)/T]\}^2}. \quad (2)$$

The corresponding fit of α_{Sch} with γ^{HS} as the only free parameter gives the dashed line in Fig. 1(b). Obviously, both fits hardly differ because the modified $\Delta_{\mathrm{Co}}^{\mathrm{HS}}$ is compensated by a larger value of $\gamma^{\mathrm{HS}}=2\%$. We note, however, that this does *not* necessarily correspond to a larger pressure dependence of Δ_{Co}^0 because α_{Sch} of Eq. (2) is determined by the pressure dependencies of Δ_{Co}^0 and that of the slope a; see, e.g., the discussions in Refs. 24, 27, and 28. In view of the small differences between both fits for LaCoO_3 and since there are no indications for a temperature-dependent Δ_{Co} from other physical quantities, the fits of α_{Sch} of the other $R\mathrm{CoO}_3$ crystals have been done for constant energy gaps only. Since Eqs. (1) and (2) are identical for $a=0$, this analysis is not able to distinguish between both models. The obtained values of Δ_{Co} and γ are given in Table I. As expected, Δ_{Co} strongly increases with decreasing radius in the R^{3+} ions and therefore the spin-state transition monotonically shifts to higher temperature. The onset temperatures T_{on} of the spin-state transitions of all compounds $T_{\mathrm{on}} \simeq 25$, 175, 230, and 400 K for R=La, Pr, Nd, and Eu, respectively, are marked by arrows in Fig. 1(b).

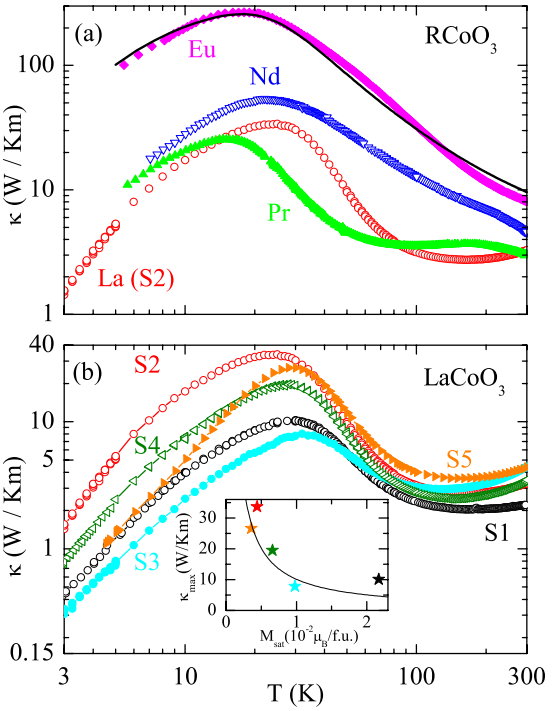

FIG. 2. (Color online) (a) Thermal conductivity of $R\mathrm{CoO}_3$ with R=La, Pr, Nd, and Eu; the solid line is a fit via Eq. (3). (b) Thermal conductivity of five different LaCoO_3 single crystals S1–S5 (note the different scale). The inset shows the maximum values of the thermal conductivity κ_{max} of these crystals vs the saturation values of the magnetization M_{sat} measured at 2 K. As shown by the solid line, we find an approximate proportionality $\kappa_{\mathrm{max}} \propto 1/M_{\mathrm{sat}}$ (see text).

B. Thermal conductivity

Figure 2(a) displays the thermal-conductivity data of $R\mathrm{CoO}_3$. As has been already found in previous studies on LaCoO_3 (Refs. 18 and 19), the overall shape and qualitative behavior of $\kappa(T)$ are rather unusual. First of all, κ is rather low in the whole temperature range and its temperature dependence clearly deviates from the typical behavior expected for a conventional phononic heat conductor. The thermal conductivity of LaCoO_3 exhibits a maximum around 20–30 K. Toward higher temperatures κ rapidly drops and features a minimum around 150 K instead of the expected $1/T$ decrease (see also Ref. 19). Qualitatively, this minimum can be traced back to the spin-state transition of LaCoO_3, which sets in close to the maximum of κ. The thermal population of the Co e_g levels induces a certain fraction of Co^{3+} ions with a larger ionic radius compared to the LS Co^{3+} ions. These randomly distributed larger Co^{3+} ions do not only cause the huge anomaly in $\alpha(T)$ but also lead to additional disorder in the lattice and therefore act as additional scattering centers for phonons. Hence, the thermal conductivity is additionally suppressed. A quantitative description will be given below.

Since the spin-state transition shifts to higher temperature when La^{3+} is replaced by smaller R^{3+} ions, the above scenario suggests that the onset of the suppression of $\kappa(T)$ of $R\mathrm{CoO}_3$ systematically shifts toward higher temperature with decreasing radius in the R^{3+} ion. Let us first consider the data

of $EuCoO_3$, which is the compound with the smallest R^{3+} ion and with the largest $\Delta_{Co} \gtrsim 2000$ K (Ref. 11). Hence, the spin-state transition should not affect the thermal conductivity below room temperature, and indeed the thermal conductivity of $EuCoO_3$ exhibits much larger values than in $LaCoO_3$. Its low-temperature maximum exceeds that of $LaCoO_3$ by about one order of magnitude. Moreover, the temperature dependence of κ of $EuCoO_3$ meets the expectation of a purely phononic heat conductor.

The thermal conductivity of $NdCoO_3$ is lower than κ of $EuCoO_3$ in the entire temperature range and, at a first glance, its overall temperature dependence seems to be consistent with a conventional phononic picture too. A closer inspection of the data yields, however, a slight slope change toward a somewhat steeper decrease in $\kappa(T)$ at ≈ 230 K, i.e., close to the onset temperature of the spin-state transition; see Fig. 1(b). This slope change supports the above proposed explanation that the spin-state transition causes additional scattering centers.

$PrCoO_3$ also exhibits an unusual temperature dependence of κ, which appears somewhat similar to that of $LaCoO_3$. Above the low-temperature maximum, $\kappa(T)$ rapidly decreases to a small value of 3.5 W/Km and remains almost temperature independent between about 80 and 175 K. Above this temperature a further decrease in κ sets in. Since this decrease starts again at the onset of the spin-state transition [see Fig. 1(b)], it is natural to attribute it to the additional scattering due to the presence of Co^{3+} ions in different spin states. In contrast, the anomalous temperature dependence of $\kappa(T)$ at lower temperature is not related to the spin-state transition and, as will be discussed separately in Sec. IV B, this anomalous feature is related to the crystal-field splitting of the $4f$ shell of Pr^{3+}.

Summarizing the presented data so far, we observe in all crystals with $T_{on} < 300$ K that this onset coincides with an additional suppression of κ. Since Δ_{Co} strongly increases with decreasing R^{3+} radius,[11,23] T_{on} also shifts toward higher temperature, and the additional suppression of the thermal conductivity is less obvious because at higher temperature the usual suppression of κ due to phonon-phonon umklapp scattering becomes more and more dominant. However, the data in Fig. 2(a) also show that κ is not only suppressed at temperatures *above* T_{on}. Instead, with an increasing size in R^{3+} a monotonic decrease in κ in the *entire* temperature range is found (here we have neglected the additional suppression of κ in $PrCoO_3$). If the spin-state transition was the only effect causing additional disorder scattering, $\kappa(T)$ should approach the "bare" phononic value below T_{on}. Taking $EuCoO_3$ with stable LS Co^{3+} ions up to above room temperature as a rough measure for this "bare" phononic heat conduction, it becomes clear that this expectation is not observed in our data.

In general, the magnitude of the low-temperature maximum of κ depends on the sample quality, which determines the maximum free path. Thus, the different values within the $RCoO_3$ series could arise from different sample qualities. However, there is no indication for a systematic increase in the crystal quality with decreasing R^{3+} ion radius.[29] In order to study a possible influence of the crystal quality, we measured κ of five different $LaCoO_3$ single crystals. As shown in Fig. 2(b) the high-temperature behavior is essentially the same for all crystals, but the low-temperature maxima differ considerably. Nevertheless, all of them remain much lower than that of $EuCoO_3$. We relate the low-temperature maxima of κ to the defect concentrations by considering the low-temperature magnetization since a really pure $LaCoO_3$ with all Co^{3+} ions in the LS state would be nonmagnetic (apart from core diamagnetism and Van Vleck paramagnetism). At 2 K we measured the magnetization up to 14 T in order to reach its saturation M_{sat}, which is a measure of the content of magnetic impurities. The inset of Fig. 2 displays the low-temperature maxima of $\kappa(T)$ vs M_{sat}, which indeed roughly follow a $1/M_{sat}$ dependence as shown by the solid line.

The most likely source for magnetic impurities in $LaCoO_3$ is a weak oxygen nonstoichiometry, which changes the average valence from Co^{3+} toward Co^{2+} or Co^{4+}. Due to the odd number of $3d$ electrons, the latter are magnetic in all possible electronic configurations; but in most cases, Co^{2+} and Co^{4+} realize $t_{2g}^5 e_g^2$ and $t_{2g}^5 e_g^0$ states with spin $S=3/2$ and $S=1/2$, respectively. Experimental evidence for a weak charge-carrier doping in nominally pure $LaCoO_3$ stems from the large values of different signs of the room-temperature thermopower for the different $LaCoO_3$ crystals; cf. Table I and the discussion in Ref. 19. From the magnetization data on Sr-doped $LaCoO_3$, it is known that low doping concentrations induce so-called high-spin polarons with effective spin values up to $S=16$ (Ref. 30). Such polarons are formed around the doping-induced Co^{4+} ions, which cause a spin-state transition in the adjacent Co^{3+} ions. Most probably, this is a transition from the LS to an IS state because the electronic configuration $t_{2g}^5 e_g^1$ of Co^{3+} is favorable for the hopping of the e_g electron for both kinds of neighbors Co^{4+} with $t_{2g}^5 e_g^0$ and Co^{2+} with $t_{2g}^5 e_g^2$. Other possible configurations often only allow a t_{2g} hopping or may cause the so-called spin-blockade effect.[31,32] The formation of high-spin polarons will depend on Δ_{Co} between the LS ground and the excited spin states of Co^{3+}. Since Δ_{Co} strongly increases with decreasing R^{3+} radius, the occurrence of such polarons in the $RCoO_3$ series should get more and more unlikely for smaller R^{3+} ions. Unfortunately, the presence of high-spin polarons in $PrCoO_3$ and $NdCoO_3$ cannot be studied by magnetization measurements because of the strong magnetism of the partially filled $4f$ shells of Pr^{3+} and Nd^{3+}. For $EuCoO_3$ such an analysis is again easier because Eu^{3+} only exhibits Van Vleck paramagnetism and, in fact, the impurity contribution to the magnetic susceptibility in $EuCoO_3$ is one order of magnitude smaller than in $LaCoO_3$ (Ref. 11). Moreover, the magnetic impurity contribution of the $La_{1-x}Eu_xCoO_3$ series systematically decreases with increasing x, i.e., with decreasing average ionic size on the La site and with increasing Δ_{Co} (Ref. 11). These observations strongly support the above idea that the systematic dependence of the low-temperature thermal conductivity of $RCoO_3$ on the ionic size of R^{3+} is related to phonon scattering by high-spin polarons, whose formation depends on a weak oxygen nonstoichiometry and on Δ_{Co}.

IV. QUANTITATIVE ANALYSIS OF THE THERMAL CONDUCTIVITY

For a quantitative analysis of the thermal conductivity we use an extended Debye model[33]

$$\kappa(T) = \frac{k_B^4 T^3}{2\pi^2 \hbar^3 v_s} \int_0^{\Theta_D/T} \tau(x,T) \frac{x^4 e^x}{(e^x - 1)^2} dx. \quad (3)$$

Here, Θ_D denotes the Debye temperature, v_s is the sound velocity, ω is the phonon frequency, and $x = \hbar\omega/k_B T$ and $\tau(x,T)$ is the phonon relaxation time. The scattering rates of different independent scattering mechanisms sum up to a total scattering rate

$$\tau^{-1}(x,T) = \tau_{bd}^{-1} + \tau_{pt}^{-1} + \tau_{um}^{-1} = \frac{v_s}{L} + P\omega^4 + UT\omega^3 \exp\left(\frac{\Theta_D}{uT}\right). \quad (4)$$

The three terms on the right-hand side refer to the typical scattering rates for phonon heat transport in insulators, namely, boundary (τ_{bd}; $L=1$ mm is the characteristic length scale of the sample[34] and was kept fixed for all crystals), point defect (τ_{pt}), and phonon-phonon umklapp scattering (τ_{um}). Since the lattice spacing is a natural lower limit for the mean-free path, $\kappa(T)$ is expected to approach a minimum value at higher temperatures. In order to model this, $\tau(x,T)$ in Eq. (4) is replaced by $\max\{\tau_\Sigma(x,T), \ell_{min}/v_s\}$ with the minimum mean-free path ℓ_{min} being of the order of the lattice constant; compare the discussion in Ref. 35.

As shown by the solid line in Fig. 2, the thermal conductivity data of $EuCoO_3$ can be reproduced reasonably well by Eq. (3). In order to reduce the number of adjustable parameters, we used $\Theta_D = 600$ K and $v_s = 3900$ m/s determined for $LaCoO_3$ (Refs. 22 and 36). The other parameters have been adjusted to fit the experimental data. We obtain $P = 3.7 \times 10^{-43}$ s^3, $U = 4.9 \times 10^{-31}$ s^2/K, and $u = 7.6$; ℓ_{min} is not reached in $EuCoO_3$ up to 300 K.

A. Scattering related to the spin-state transition

In the following analysis we consider the thermal conductivity of $EuCoO_3$ as the bare phononic heat conductivity that is not influenced by the spin-state transition. For the other members of the $RCoO_3$ series, we introduce an additional scattering mechanism arising from the thermal occupation of the Co^{3+} e_g shells, which causes additional lattice disorder due to the presence of smaller and larger Co^{3+} ions in the LS and in the excited spin states, respectively. Considering the Co^{3+} ions of different sizes as pointlike defects, we assume a ω^4 frequency dependence for this additional scattering rate [cf. Eq. (4)]

$$\tau_{dis}^{-1} = Cf(T)\omega^4, \quad (5)$$

where C is an adjustable parameter describing the scattering strength and $f(T)$ models the temperature dependence of the additional lattice disorder.

The unknown functions $Cf(T)$ for $LaCoO_3$, $PrCoO_3$, and $NdCoO_3$ can be calculated from the experimental data in the following way: We use Eq. (4) with all the parameters obtained from the fit of κ of $EuCoO_3$ kept fix and add τ_{dis}^{-1}. Then the total τ is used in Eq. (3), and the values of $Cf(T)$ at each temperature are determined point by point from the measured $\kappa(T)$. The resulting $Cf(T)$ curves for all three $RCoO_3$ samples are shown by the open symbols in Fig. 3. In order to avoid additional complications arising from the aforementioned high-spin polarons, we restrict the analysis to the temperature range above 25 K. For $LaCoO_3$ the resulting $Cf(T)$ has a pronounced maximum around 100 K and strongly resembles the temperature dependence of the magnetic susceptibility of $LaCoO_3$. Here, we have used sample S2, which exhibits the highest value of the low-temperature maximum of κ, i.e., the sample, which is least affected by impurity scattering. We note, however, that in the considered temperature range above 25 K the resulting $Cf(T)$ is not very different for the other $LaCoO_3$ crystals. For $PrCoO_3$, $Cf(T)$ features a clear maximum followed by a slope change around 175 K. The obtained values of $Cf(T)$ for $NdCoO_3$ are much lower than those of $LaCoO_3$ and $PrCoO_3$ and there is no maximum, but again a clear slope change around $T_{on} \simeq 230$ K. Thus, we find in all three $RCoO_3$ compounds either an increase in $Cf(T)$ or a slope change toward larger values at temperatures close to the respective onset temperatures of the spin-state transition; see Fig. 1.

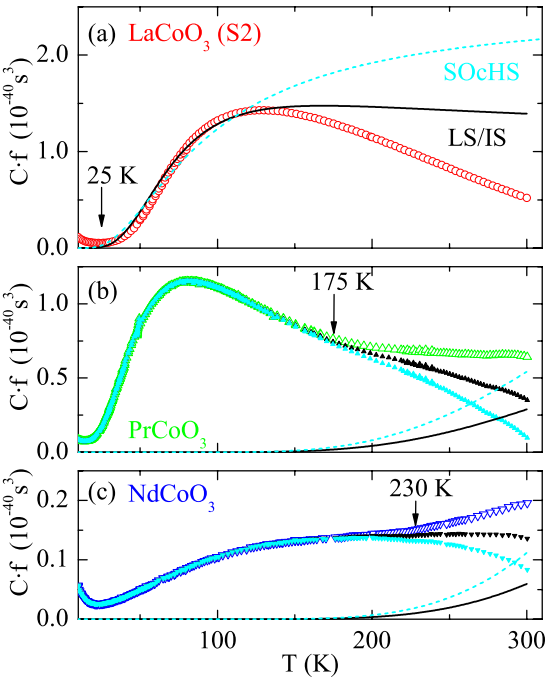

FIG. 3. (Color online) Open symbols denote the experimentally obtained additional scattering rates $Cf(T)$, which are needed to suppress κ from a hypothetical bare phonon heat conductivity represented by κ of $EuCoO_3$ to the measured values of κ of $LaCoO_3$, $PrCoO_3$, and $NdCoO_3$ (see text for details). In all three $RCoO_3$ an additional scattering sets in above the respective onset temperature T_{on} (marked by the arrow in each panel) of the spin-state transition. The lines show the expected additional scattering rates due to the spin-state transition for a LS/IS scenario (solid) and for the SOcHS model (dashed); see Eqs. (5) and (6). In panel (a) the scattering strengths C for each model have been adjusted by fitting the lines to the experimental data in the temperature range below 150 K. These values have been kept fixed to calculate the lines in panels (b) and (c), and, as shown by the solid symbols, the additional scattering above T_{on} completely vanishes when these lines are subtracted from the experimental $Cf(T)$.

In order to model the additional scattering rate we use the so-called Nordheim rule,[37] which is a successful approach to

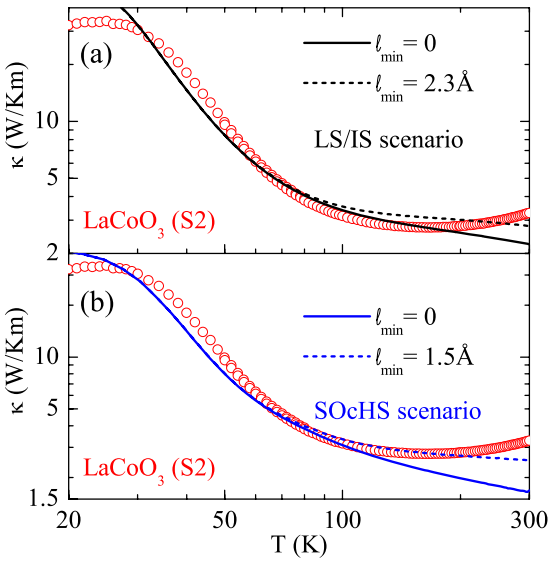

FIG. 4. (Color online) Thermal conductivity (symbols) of $LaCoO_3$ with fits based on Eq. (3) assuming (a) the LS-IS or (b) the SOcHS model for the spin-state transition. The dashed (solid) lines are obtained when a minimum mean free ℓ_{min} is (is not) taken into account (see text).

describe κ in disordered mixed alloys. There, the additional scattering rate is proportional to $x(1-x)$ with x being the fraction of one of the constituents. In the present case this corresponds to the fractions $n_{IS/HS}$ of Co^{3+} ions in the higher and $n_{LS}=(1-n_{IS/HS})$ in the LS states. Thus, the temperature dependence of the additional scattering rate of Eq. (5) is expected to be given by [see Eqs. (1) and (2)]

$$f(T) = \frac{\nu \exp[-\Delta_{Co}(T)/T]}{\{1+\nu \exp[-\Delta_{Co}(T)/T]\}^2}. \quad (6)$$

The solid line in Fig. 3(a) corresponds to a calculation of $Cf(T)$ via Eq. (6) using the temperature independent $\Delta_{Co}=185$ K of the LS-IS scenario. Here, C is the only adjustable parameter, and for $C=5.9\times10^{-40}$ s^3 this model yields a good description of the experimental data in the temperature range from 30 to 150 K. The dashed line shows the corresponding fit (yielding $C=11\times10^{-40}$ s^3) for the same temperature range based on the SOcHS scenario with a temperature-dependent $\Delta_{Co}(T)$, which is in reasonable agreement with the data too. Obviously, both models are not able to describe the decrease in $f(T)$ above 150 K. This disagreement, however, does not contradict the models because for $T\gtrsim150$ K the measured κ of $LaCoO_3$ is already close to its minimum value arising from the aforementioned lower limit of the mean-free path. For $Cf(T)$ of $PrCoO_3$ and $NdCoO_3$, we keep the values of C fixed and use the gap values $\Delta_{Co}=1200$ and 1700 K obtained from the analysis of $\alpha(T)$; cf. Table I. The corresponding curves, which for the different models only differ in the scattering strengths, are shown as solid and dashed lines in Figs. 3(b) and 3(c). When we subtract these lines from the experimental data, the slope changes around T_{on} completely vanish as is shown by the solid symbols in Figs. 3(b) and 3(c). This gives further evidence that the spin-state transition is indeed responsible for the suppression of the thermal conductivity of $PrCoO_3$ and $NdCoO_3$ as it is the case for $LaCoO_3$.

Encouraged by this finding we tried to fit the thermal conductivity of $LaCoO_3$ via Eq. (3) including the additional scattering rate given by Eqs. (5) and (6) in Eq. (4). Again, we restrict our analysis to $T\gtrsim25$ K and keep most of the fit parameters fixed to their values as obtained from the Debye fit of the bare phononic κ of $EuCoO_3$. From these parameters, we only readjust the prefactor P of the point-defect scattering term in Eq. (4) because the number of point defects varies in different crystals, and point-defect scattering also reduces κ at high temperatures. In addition, the scattering strength C is readjusted but changes only little (to $C=6\times10^{-40}$ s^3 and 12×10^{-40} s^3 for the LS/IS and the SOcHS models, respectively), and we consider the minimum mean-free path ℓ_{min}. The results for the LS-IS as well as the SOcHS model are displayed in Fig. 4. Both models describe the thermal conductivity well over a large temperature range of about 200 K, in particular, when the minimum mean-free path is taken into account. As was already seen in Fig. 3 the quality of the fits based on the different models hardly differs. Therefore, the analysis of the thermal conductivity of $RCoO_3$ does not allow to judge whether the LS/IS or the SOcHS scenario is preferable.

B. Scattering related to crystal-field excitations

Next we consider the additional suppression of κ of $PrCoO_3$ below T_{on}, which is not related to the spin-state transition. As can be seen in Fig. 1, the thermal expansion of this compound also exhibits an additional anomaly at lower temperatures. This anomaly arises from the crystal-field splitting of the $4f$ shell of the Pr^{3+} ions. In an orthorhombic crystal field, the $^3H_4$ multiplet of the free Pr^{3+} ion splits into nine singlets. We are not aware of experimental investigations of the crystal-field splitting in $PrCoO_3$, but it is known that the crystal-field levels of other orthorhombic $PrAO_3$ are very similar.[38–40] Only the lower levels slightly depend on the exact orthorhombic distortion, which is mainly characterized by the $A-O-A$ canting angle. The energy splitting between the crystal-field ground state and the first-excited level in $PrCoO_3$ can be determined from a fit of the low-temperature thermal expansion by a Schottky anomaly. As shown in Fig. 5(a), such a fit for two nondegenerate levels [setting $\nu=1$ and replacing Δ_{Co} by Δ_{CF} in Eq. (1)] describes the experimental data well and yields $\Delta_{CF}=E_1=70$ K and $\gamma=0.056\%$. For the higher-lying energy levels we use the values $E_2=151$ K, $E_3=174$ K, and $E_3=235$ K,… of $PrNiO_3$ (Ref. 40), which has almost the same $A-O-A$ canting angle as $PrCoO_3$. We note here that the thermal population of these higher-lying levels may contribute to $\alpha(T)$ at higher temperatures; but below about 50 K, the two-level system used is sufficient to model the experimental data.

The most likely source for the suppression of the thermal conductivity of $PrCoO_3$ in the intermediate temperature range is resonant scattering between different $4f$ crystal-field levels as it is also known from, e. g., rare-earth garnets.[41] In such a resonant scattering process, a phonon is absorbed by

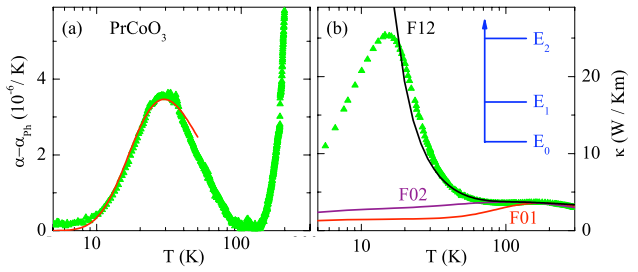

FIG. 5. (Color online) Low-temperature (a) thermal expansion and (b) thermal conductivity of $PrCoO_3$. The thermal-expansion data (symbols) in panel (a) are well described by a Schottky anomaly (line) of a two-level system with nondegenerate levels with energy splitting $E_1-E_0=70$ K. The lines F01, F02, and F12 in panel (b) are fits for $T>20$ K to the thermal-conductivity data (symbols) including either the resonant scattering process $E_0 \leftrightarrow E_1$, $E_0 \leftrightarrow E_2$, or $E_1 \leftrightarrow E_2$, respectively. A sketch of the energy levels is also included (Ref. 40).

inducing a transition between different energy levels and then re-emitted in an arbitrary direction (see, e.g., Refs. 41–43) causing an additional thermal resistance. A mechanism based on random volume changes (as discussed above for the Co^{3+} spin-state transition) is unlikely because the $4f$ orbitals are inner shells. This difference is directly reflected in the magnitudes of the Schottky peaks, which are mainly determined by the underlying volume change. As can be seen in Fig. 1, the low-temperature peak in α of $PrCoO_3$ is, e.g., one order of magnitude smaller than that of $LaCoO_3$ (Ref. 44).

In order to model $\kappa(T)$ in the low-T range, we include the additional scattering rate

$$\tau_{\mathrm{res}}^{-1} = R\frac{4\omega^4\Delta_{\mathrm{CF}}^4}{(\Delta_{\mathrm{CF}}^2-\omega^2)^2}(N_i+N_j) \tag{7}$$

in Eq. (4) describing a direct resonant scattering process.[42,45] Here, $\Delta_{\mathrm{CF}}=|E_i-E_j|$ is the energy difference between the two levels, and N_i and N_j denote their population determined by the partition sum. For the fit we keep again $\Theta_{\mathrm{D}}=600$ K and $v_s=3900$ m/s, while P, U, u, and R are adjusted with respect to the data. The fits have been restricted to $T\geq 20$ K since other processes may become dominant at very low temperatures.

In a first attempt, resonant scattering between E_0 and the first-excited level E_1 is considered yielding the fit labeled F01 in Fig. 5(b). This fit only reproduces the data for $T \gtrsim 100$ K but totally misses the low-temperature maximum in $\kappa(T)$. Basically the same result is achieved by considering the process $E_0 \leftrightarrow E_2$ [curve F02 in Fig. 5(b)]. A much better description of the data is obtained however for the process $E_1 \leftrightarrow E_2$ (curve F12 with parameters $P=5\times10^{-43}$ s^3, $U=4.85\times10^{-18}$ s^2/K, $u=5$, and $R=3.8\times10^{-40}$ s^3). Hence, the transition $E_1 \leftrightarrow E_2$ appears to be the dominant scattering channel of the phonons in $PrCoO_3$ at intermediate temperatures.

Finally, we comment on the presence (absence) of a Schottky anomaly of $\alpha(T)$ in $PrCoO_3$ ($NdCoO_3$). Because there are no studies of the crystal-field levels of $RCoO_3$, we use the values of the structurally similar $RNiO_3$ series, whose crystal-field levels have been studied in detail.[40] The excited levels of $NdNiO_3$ are at $E_1=130$ K, $E_2=220$ K,…, i.e., clearly higher than those of $PrNiO_3$. Apart from this quantitative difference, the Pr^{3+} and Nd^{3+} crystal-field levels also qualitatively differ: the former are singlets while the latter are Kramers doublets because of the even and odd number of $4f$ electrons, respectively. Nevertheless, one expects Schottky peaks for both compounds, which in the low-temperature regime ($T \ll E_2$) can be approximated by a simple two-level system with energy splitting $\Delta=E_1$. The corresponding Schottky anomaly of the specific heat is fully determined by E_1 and by the degeneracies of the two levels. As a consequence, the Schottky anomaly of Nd^{3+} is broadened compared with that of Pr^{3+} because it scales with T/E_1 shifting T_{max} from 30 to 55 K. For a two-level system, the Schottky anomaly of the thermal expansion α_i directly scales with that of the specific heat, but the scaling factor is given by the uniaxial pressure dependence $\partial \ln \Delta / \partial p_i$; see, e.g., Ref. 24. Thus, we conclude that the pressure dependence of E_1 of $NdCoO_3$ is too weak to cause a sizeable anomaly of $\alpha(T)$ in the temperature range up to 200 K; while for $PrCoO_3$, we obtain $\partial \ln E_1 / \partial p \simeq 9\%/\mathrm{GPa}$ for hydrostatic pressure. One may speculate that the different pressure dependencies are related to the qualitatively different crystal-field levels of Pr^{3+} and Nd^{3+}. Recently, we have also studied the thermal expansion of $NdMnO_3$ and again there was no indication of a Schottky anomaly around 55 K but we observed a Schottky anomaly around 8 K. Our analysis revealed that this Schottky anomaly arises from the ground-state doublet of Nd^{3+}, whose degeneracy is lifted already in zero magnetic field by the weak ferromagnetic moment of the Mn^{3+} spins, and the corresponding energy splitting further increases with magnetic field.[43]

V. SUMMARY

In this paper we have presented measurements of the thermal-expansion coefficient and the thermal conductivity of $RCoO_3$ with trivalent R=La, Pr, Nd, and Eu. As a consequence of the chemical pressure due to the decreasing ionic radius from R=La to Eu, the energy gap between the LS ground and the first-excited spin states of the Co^{3+} ions increases drastically, and the temperature-induced spin-state transition of the Co^{3+} ions is systematically shifted toward higher temperature. This strong pressure dependence is also reflected in pronounced Schottky anomalies in the thermal-expansion coefficients making this quantity a sensitive probe to analyze spin-state transitions. The microscopic origin of the pressure dependence is the volume change due to the partial occupation of the e_g levels of the Co^{3+} ions in the excited spin state in contrast to the empty e_g levels of LS Co^{3+} ions. Another consequence of this volume difference is a strong suppression of the phonon heat transport, which sets in above the onset temperature of the spin-state transition, because the random occupation of the Co sites with Co^{3+} ions in different spin states, i.e., of different sizes, causes additional lattice disorder. By considering this disorder as pointlike defects, our analysis clearly shows this effect in the

temperature dependence of the corresponding scattering rates of $LaCoO_3$, $PrCoO_3$, and $NdCoO_3$, where the spin-state transition sets in below room temperature in contrast to $EuCoO_3$, which exhibits a stable LS state up to about 400 K.

Quantitatively, the temperature dependence of the additional scattering due to the spin-state transition can be described in a model based on the Nordheim rule, which is usually applied to describe scattering in disordered mixed alloys. For the cobaltates, this means that the temperature dependence of this additional scattering rate is given by the product of the occupation numbers of the LS and of the excited spin states. We find the same scattering strengths for $LaCoO_3$, $PrCoO_3$, and $NdCoO_3$. Our analysis, however, does not allow to distinguish between the different models discussed for the spin-state transition in $LaCoO_3$, namely, a LS-IS scenario with a temperature-independent energy gap or the more recently proposed model based on a spin-orbit coupled high-spin state with a temperature-dependent energy gap.

The above-described model explains a damping of the phonon heat transport above the onset temperature of the spin-state transition. Experimentally, however, we find that as a function of increasing size in the R^{3+} ions the thermal conductivity decreases also in the temperature range below the respective onset of the spin-state transition. By studying five different $LaCoO_3$ single crystals, we could show that the low-temperature thermal conductivity inversely scales with the amount of magnetic impurities. Most likely, these impurities arise from a weak oxygen nonstoichiometry giving rise to a certain amount of Co^{2+} or Co^{4+} ions. Because it is known that these magnetic Co ions tend to form so-called high-spin polarons by inducing a spin-state transition in the neighboring Co^{3+} ions, our data suggest that the phonon damping at low temperature arises from such a doping-induced spin-state transition. The drastic increase in the energy gap to the excited spin state of Co^{3+} for decreasing R^{3+} ionic radii makes the formation of spin polarons more and more unlikely and thus can naturally explain the systematic increase in the thermal conductivity in the temperature range below the temperature-induced spin-state transition.

Additional low-temperature features have to be considered in $PrCoO_3$ because the thermal expansion exhibits another Schottky anomaly and there is an additional suppression of the thermal conductivity. Both effects are not related to the temperature-dependent spin-state transition of Co^{3+} but stem from the crystal-field splitting of the ground-state multiplet of the $4f$ shell of Pr^{3+}. Our analysis demonstrates that the Schottky anomaly of the thermal expansion arises from a thermal occupation of the first-excited crystal-field level; whereas, the phonon damping is a consequence of resonant phonon scattering between the first two excited crystal-field levels.

ACKNOWLEDGMENTS

We acknowledge useful discussions with M. Haverkort and A. Sologubenko. This work was supported by the Deutsche Forschungsgemeinschaft through Sonderforschungsbereich 608.

*lorenz@ph2.uni-koeln.de

[1] G. H. Jonker and J. H. Van Santen, Physica (Amsterdam) **19**, 120 (1953).
[2] J. B. Goodenough and P. M. Raccah, J. Appl. Phys. **36**, 1031 (1965).
[3] M. A. Señarís-Rodríguez and J. B. Goodenough, J. Solid State Chem. **116**, 224 (1995).
[4] T. Saitoh, T. Mizokawa, A. Fujimori, M. Abbate, Y. Takeda, and M. Takano, Phys. Rev. B **55**, 4257 (1997).
[5] K. Asai, A. Yoneda, O. Yokokura, J. M. Tranquada, G. Shirane, and K. Kohn, J. Phys. Soc. Jpn. **67**, 290 (1998).
[6] Y. Tokura, Y. Okimoto, S. Yamaguchi, H. Taniguchi, T. Kimura, and H. Takagi, Phys. Rev. B **58**, R1699 (1998).
[7] S. Yamaguchi, Y. Okimoto, and Y. Tokura, Phys. Rev. B **55**, R8666 (1997).
[8] Y. Kobayashi, N. Fujiwara, S. Murata, K. Asai, and H. Yasuoka, Phys. Rev. B **62**, 410 (2000).
[9] K. Sato, M. I. Bartashevich, T. Goto, Y. Kobayashi, M. Suzuki, K. Asai, A. Matsuo, and K. Kindo, J. Phys. Soc. Jpn. **77**, 024601 (2008).
[10] C. Zobel, M. Kriener, D. Bruns, J. Baier, M. Grüninger, T. Lorenz, P. Reutler, and A. Revcolevschi. Phys. Rev. B **66**, 020402(R) (2002).
[11] J. Baier, S. Jodlauk, M. Kriener, A. Reichl, C. Zobel, H. Kierspel, A. Freimuth, and T. Lorenz, Phys. Rev. B **71**, 014443 (2005).
[12] S. Noguchi, S. Kawamata, K. Okuda, H. Nojiri, and M. Motokawa, Phys. Rev. B **66**, 094404 (2002).
[13] M. W. Haverkort, Z. Hu, J. C. Cezar, T. Burnus, H. Hartmann, M. Reuther, C. Zobel, T. Lorenz, A. Tanaka, N. B. Brookes, H. H. Hsieh, H. J. Lin, C. T. Chen, and L. H. Tjeng, Phys. Rev. Lett. **97**, 176405 (2006).
[14] A. Podlesnyak, S. Streule, J. Mesot, M. Medarde, E. Pomjakushina, K. Conder, A. Tanaka, M. W. Haverkort, and D. I. Khomskii, Phys. Rev. Lett. **97**, 247208 (2006).
[15] T. Kyômen, Y. Asaka, and M. Itoh, Phys. Rev. B **67**, 144424 (2003).
[16] M. Kriener, C. Zobel, A. Reichl, J. Baier, M. Cwik, K. Berggold, H. Kierspel, O. Zabara, A. Freimuth, and T. Lorenz, Phys. Rev. B **69**, 094417 (2004).
[17] M. Kriener, M. Braden, H. Kierspel, D. Senff, O. Zabara, C. Zobel, and T. Lorenz, arXiv:0801.4188 (unpublished).
[18] J.-Q. Yan, J.-S. Zhou, and J. B. Goodenough, Phys. Rev. B **69**, 134409 (2004).
[19] K. Berggold, M. Kriener, C. Zobel, A. Reichl, M. Reuther, R. Müller, A. Freimuth, and T. Lorenz, Phys. Rev. B **72**, 155116 (2005).
[20] K. Berggold, T. Lorenz, J. Baier, M. Kriener, D. Senff, H. Roth, A. Severing, H. Hartmann, A. Freimuth, S. Barilo, and F. Nakamura, Phys. Rev. B **73**, 104430 (2006).

[21] R. Pott and R. Schefzyk, J. Phys. E **16**, 444 (1983).
[22] S. Stølen, F. Grønvold, H. Brinks, T. Atake, and H. Mori, Phys. Rev. B **55**, 14103 (1997).
[23] S. Yamaguchi, Y. Okimoto, and Y. Tokura, Phys. Rev. B **54**, R11022 (1996).
[24] T. Lorenz, S. Stark, O. Heyer, N. Hollmann, A. Vasiliev, A. Oosawa, and H. Tanaka, J. Magn. Magn. Mater. **316**, 291 (2007).
[25] T. Lorenz, O. Heyer, M. Garst, F. Anfuso, A. Rosch, C. Rüegg, and K. Krämer, Phys. Rev. Lett. **100**, 067208 (2008).
[26] K. Asai, O. Yokokura, M. Suzuki, T. Naka, T. Matsumoto, H. Takahashi, N. Môri, and K. Kohn, J. Phys. Soc. Jpn. **66**, 967 (1997).
[27] N. Johannsen, A. Vasiliev, A. Oosawa, H. Tanaka, and T. Lorenz, Phys. Rev. Lett. **95**, 017205 (2005).
[28] F. Anfuso, M. Garst, A. Rosch, O. Heyer, T. Lorenz, C. Rüegg, and K. Krämer, Phys. Rev. B **77**, 235113 (2008).
[29] One may speculate that the low-temperature maximum of κ is also influenced by twinning. All these single crystals are twinned, but it seems plausible that the average size of the twin domains increases from $LaCoO_3$ to $EuCoO_3$ because the deviation from the cubic symmetry increases. However, the observed correlation between κ_{max} and the magnetic impurity concentration for the different $LaCoO_3$ crystals makes it rather unlikely to explain the different low-temperature maxima of κ in terms of different domain sizes.
[30] S. Yamaguchi, Y. Okimoto, H. Taniguchi, and Y. Tokura, Phys. Rev. B **53**, R2926 (1996).
[31] A. Maignan, V. Caignaert, B. Raveau, D. Khomskii, and G. Sawatzky, Phys. Rev. Lett. **93**, 026401 (2004).
[32] R. Lengsdorf, M. Ait-Tahar, S. S. Saxena, M. Ellerby, D. I. Khomskii, H. Micklitz, T. Lorenz, and M. M. Abd-Elmeguid. Phys. Rev. B **69**, 140403(R) (2004).
[33] R. Bermann, *Thermal Conduction in Solids* (Clarendon, Oxford, 1976).
[34] S. Y. Li, J. B. Bonnemaison, A. Payeur, P. Fournier, C. H. Wang, X. H. Chen, and L. Taillefer, Phys. Rev. B **77**, 134501 (2008).
[35] K. Kordonis, A. V. Sologubenko, T. Lorenz, S. W. Cheong, and A. Freimuth, Phys. Rev. Lett. **97**, 115901 (2006).
[36] S. Murata, S. Isida, M. Suzuki, Y. Kobayashi, K. Asai, and K. Kohn, Physica B (Amsterdam) **263-264**, 647 (1999).
[37] L. Nordheim, Ann. Phys. **401**, 641 (1931).
[38] K. Feldmann, K. Hennig, L. Kaun, B. Lippold, M. M. Lukina, S. Matthies, W. Matz, and E. Warming, Phys. Status Solidi B **72**, 817 (1975).
[39] A. Podlesnyak, S. Rosenkranz, F. Fauth, W. Marti, H. J. Scheel, and A. Furrer, J. Phys.: Condens. Matter **6**, 4099 (1994).
[40] S. Rosenkranz, M. Medarde, F. Fauth, J. Mesot, M. Zolliker, A. Furrer, U. Staub, P. Lacorre, R. Osborn, R. S. Eccleston, and V. Trounov, Phys. Rev. B **60**, 14857 (1999).
[41] G. A. Slack and D. W. Oliver, Phys. Rev. B **4**, 592 (1971).
[42] M. Hofmann, T. Lorenz, G. S. Uhrig, H. Kierspel, O. Zabara, A. Freimuth, H. Kageyama, and Y. Ueda, Phys. Rev. Lett. **87**, 047202 (2001).
[43] K. Berggold, J. Baier, D. Meier, J. A. Mydosh, T. Lorenz, J. Hemberger, A. Balbashov, N. Aliouane, and D. N. Argyriou, Phys. Rev. B **76**, 094418 (2007).
[44] We also mention that our attempts to describe the additional damping of κ due to the spin-state transition of $LaCoO_3$ by a resonant scattering process completely failed.
[45] R. Orbach, Proc. Phys. Soc. Jpn. **77**, 821 (1961).